

Suppl. Figure 1. Related to Figure 1 and 2.

Suppl. Figure 1. Related to Figure 1 and 2.

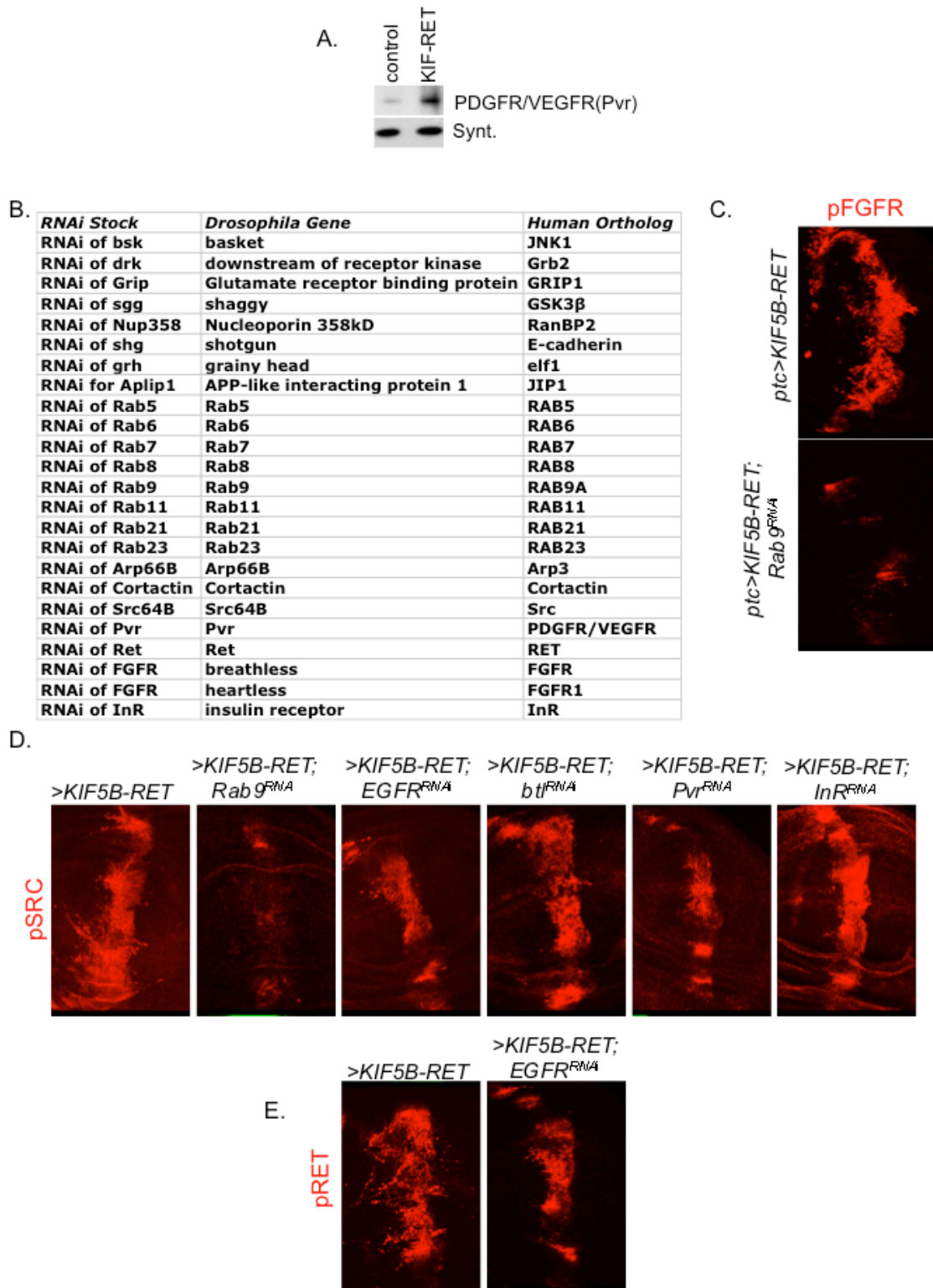
(A-C) Bright field images of adult wings of the indicated genotype. Uniform expression of human *KIF5B-RET* ($765>hKIF5B-RET$) in developing discs resulted in adults wings with ectopic wing veins (B; asterisks) compared to controls (A). Expression of activating point mutant RET, $765>dRET^{M955T}$ (C) led to a weaker wing vein phenotype.

(D) Third instar larval wing epithelia, *en face* view. Expression of *Drosophila* ortholog of activating RET point mutant in a central stripe of larval wing epithelial cells ($ptc>dRET^{M955T}$, marked by eGFP expression) did not lead to pEGFR upregulation.

(E) Graphic representation of structural domains of the human *KIF5B-RET* transgene used in our studies. MD, motor; CC, coiled-coil; K, kinase; TM, transmembrane; Cad, Cadherin repeats; Cys, cysteine rich region. Inverted shaded triangle indicates breakpoints within RET and KIF5B genes and point of fusion.

(F) Expression of *KIF5B-RET* ($ptc>hKIF5B-RET$) in a central stripe of larval wing epithelial cells led to strong expression of EGFR activity reporter *pnt-lacZ* (G) compared to controls (F).

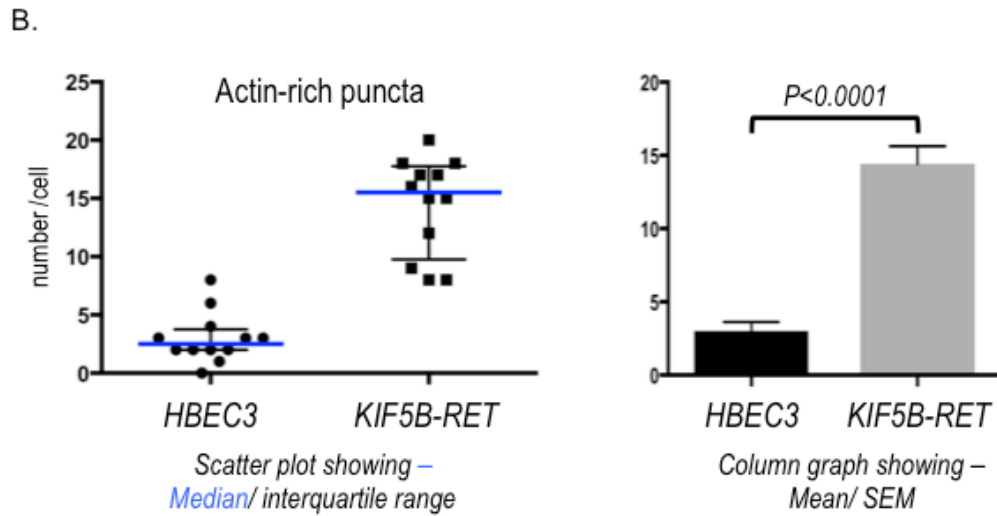
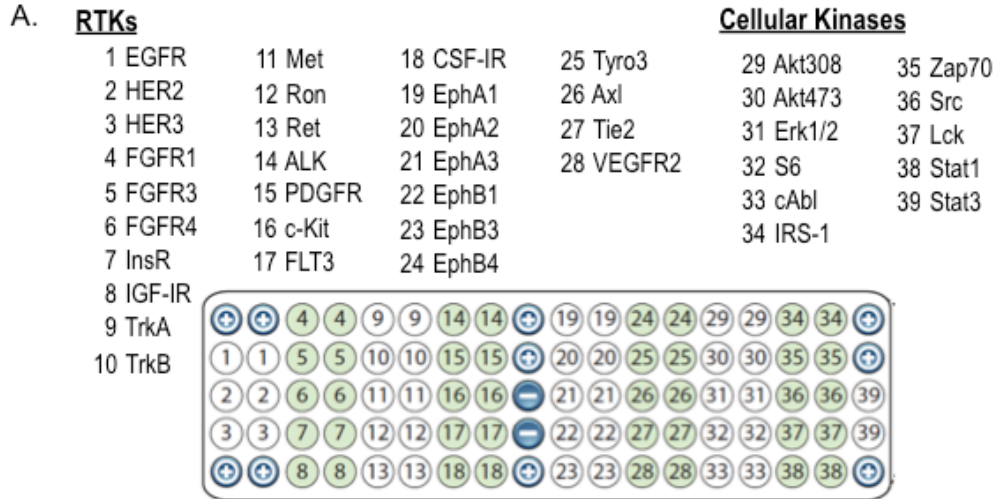
(H-K) EGFR activation is functionally linked to KIF5B-RET expression. The indicated transgenes were expressed under the control of the *ptc-GAL4* driver, e.g., $ptc>KIF5B-RET$, and adult wings were analyzed for abnormal wing vein pattern. (H) Control adult wing; white box indicates where *ptc* promoter is active during earlier larval stages. (I) $ptc>KIF5B-RET$ adult wings showing thickening of wing vein (asterisk). (J) Expression of *Drosophila* oncogenic variant $ptc>dRET^{M955T}$ showed no ectopic vein material. (K) Expressing RNA interference transgene targeting EGFR in KIF5B-RET expressing cells, $ptc>KIF5B-RET$, *EGFR^{RNAi}*, suppressed the ectopic wing vein phenotype. (L-M) $ptc>KIF5B-RET$ cells show strong upregulation of JNK pathway reporter TRE-RFP (M). Control cells show background levels of activity of the same reporter (L).



Suppl. Figure 2. Related to Figure 3 and 4.

Suppl. Figure 2. Related to Figure 3 and 4.

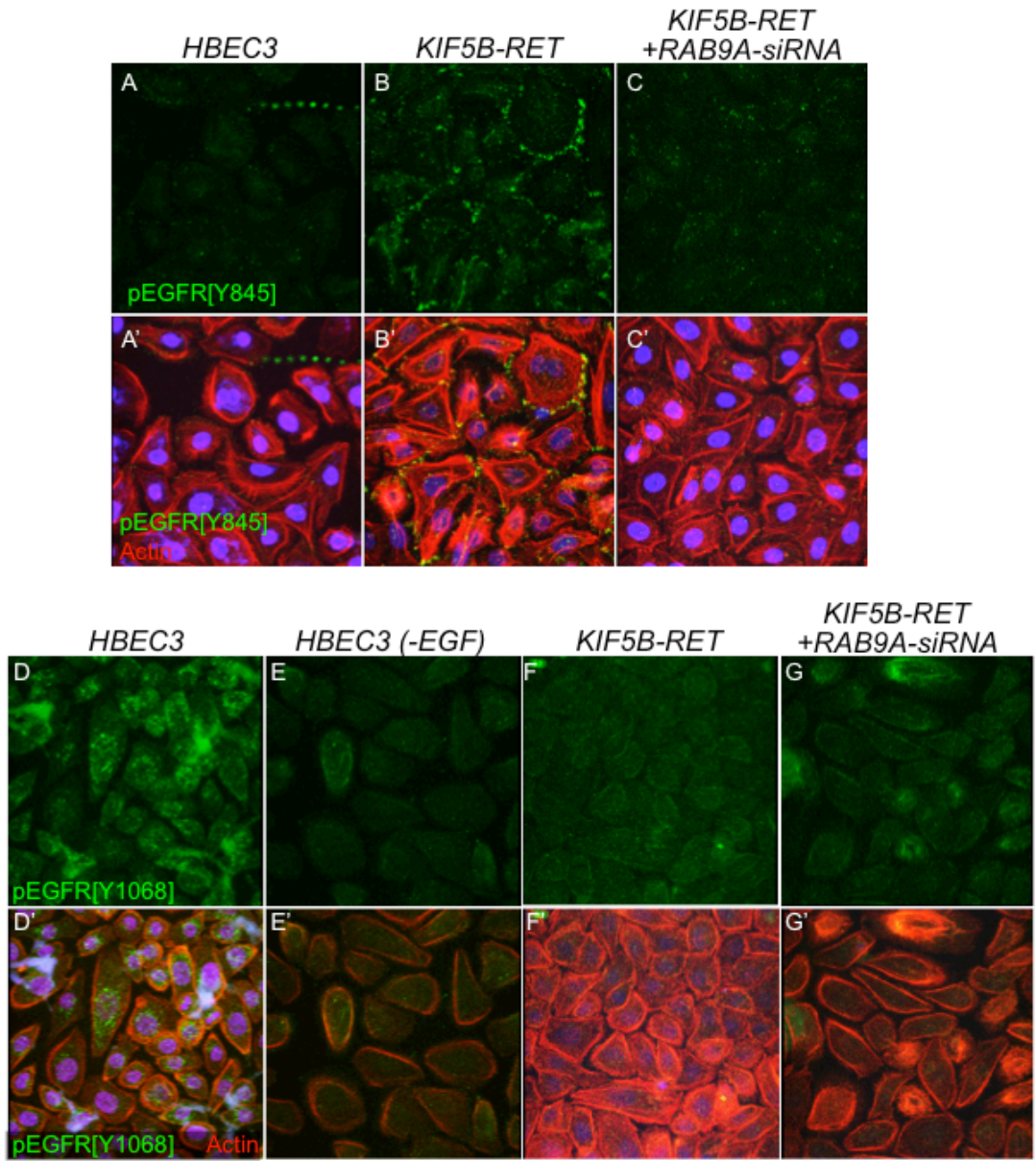
(A) Western blot analysis indicating elevated levels of Drosophila PDGFR/VEGFR ortholog Pvr in developing wing discs (*765>KIF5B-RET*) expressing *KIF5B-RET*; Syntaxin was used as loading control. (B) Table showing *Drosophila* TRIP-RNAi knockdown lines used to assess effect of targeted knockdown on viability of *ptc>KIF5B-RET* flies and effect on pEGFR activation within the *ptc* domain. The name of the *Drosophila* gene and its corresponding human ortholog is indicated. (C) *ptc>KIF5B-RET* larval wing discs showing effect of *Rab9^{RNAi}* knockdown on levels of pFGFR. In *ptc>GFP, KIF5B-RET* wing discs, almost all discs showed strong activation of pFGFR (Fig 4). Simultaneous knockdown of Rab9 (*ptc>GFP, KIF5B-RET, Rab9^{RNAi}*) reduced the number of discs showing high pFGFR activation. (D) In *ptc>KIF5B-RET* larval wing discs simultaneous knockdown of Rab9 (*ptc>GFP, KIF5B-RET, Rab9^{RNAi}*) reduced pSRC levels considerably. But in *KIF5B-RET* expressing larval wing discs knockdown of individual RTK's (see Fig 5A) did not alter pSRC levels significantly. (E) Simultaneous knockdown of EGFR in *KIF5B-RET* larval wing discs (*ptc>GFP, KIF5B-RET, EGFR^{RNAi}*) did not alter the levels of pRET significantly.



Suppl. Figure 3. Related to Figure 5.

Suppl. Figure 3. Related to Figure 5.

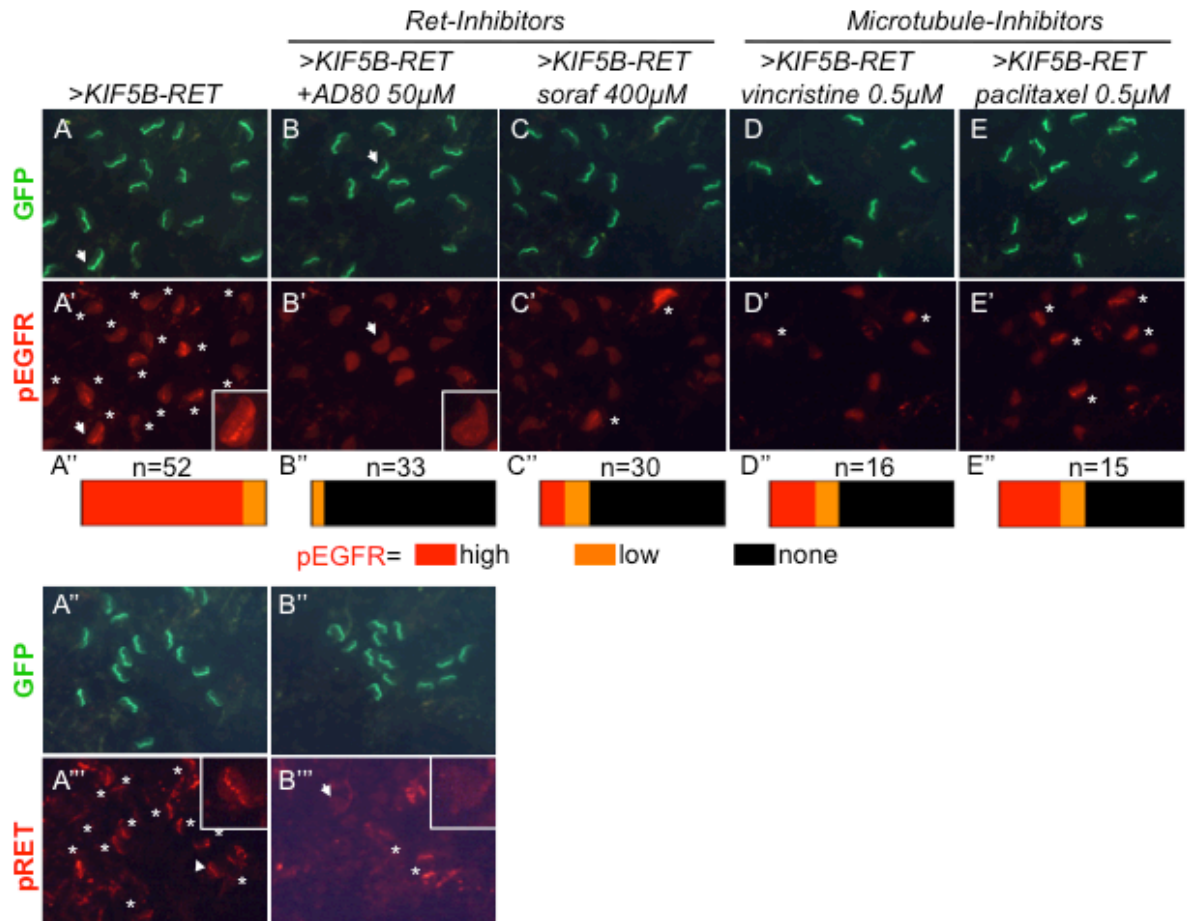
(A) Cell Signaling RTK Array. Numbers and names correspond to pictorial representation of phospho-antibody spots on the array. (B) Quantification of the number of Actin-rich puncta assessed by Phalloidin-Rhodamine staining of *HBEC3[KIF5B-RET]* cells compared to parental *HBEC3* cells. Confocal images 63x of cells were analyzed as full overlay covering entire thickness of the cells. Left Panel: Actin-rich puncta in Fig. 6 (*e.g.*, arrows) was counted and represented as number of cells in a scatter plot using PRISM software. Right Panel: Same analysis as B represented as column graph indicating mean for each column with error bars showing SEM. Significance established by performing student t-test with Welch's correction.



Suppl. Figure 4. Related to Figure 5 and 6.

Suppl. Figure 4. Related to Figure 5 and 6.

(A-C) Immunofluorescence images showing strong upregulation of pEGFR[Y845] levels in *KIF5B-RET* cells (B) compared to parental cells (A). siRNA-mediated knockdown of *RAB9A* (C) suppressed the increase of pEGFR[Y845] levels in *KIF5B-RET* cells. DAPI labels nuclei and Phalloidin-Rhodamine labels Actin cytoskeleton. (D-E) Parental HBEC3 cells showed high levels of pEGFR[Y1068] signal, indicative of high dpERK/MAPK signaling (D). This signal is strongly suppressed if EGF is removed from the growth media (E), indicating that pEGFR[Y1068] was induced by EGF signaling. (F-G) *HBEC3[KIF5B-RET]* cells exhibited strongly reduced pEGFR[Y1068], indicating a switch away from dpERK/MAPK signaling (F). siRNA mediated knockdown of *RAB9A* partially restored pEGFR[Y1068] signal, indicating reactivation of dpERK/MAPK signaling (G; also see Fig. 7I).



Suppl. Figure 5. Related to Figure 7.

Suppl. Figure 5. Related to Figure 7.

(A-E) Inhibiting EGFR signaling is optimal for therapeutics targeting KIF5B-RET network. Immunofluorescence images of a cohort of *Drosophila* larval wing discs showing effect of RET and microtubule inhibitors on pEGFR and pRET activation by *KIF5B-RET*. In *KIF5B-RET* expressing wing discs, *ptc>eGFP, KIF5B-RET*, almost all discs showed activation of pEGFR (A', asterisk). The polypharmacological kinase inhibitor AD80 strongly suppressed pEGFR activation (B) while clinically approved drug sorafenib was moderately effective (C). Microtubule/cytoskeleton inhibitors vincristine and paclitaxel were also somewhat effective. Binned representation of relative number of discs showing high, low, and no pEGFR expression (A'', B'', C'', D'', E''). The GFP channel for each genotype (A, B, C, D, E) shows region of the wing disc where transgenes were activated and match regions where pEGFR activation occurs. Inset shows examples of wing discs in images marked by white arrowhead. pRET activation by *KIF5B-RET* and its inhibition by AD80 shown in panels (A'''- B''').

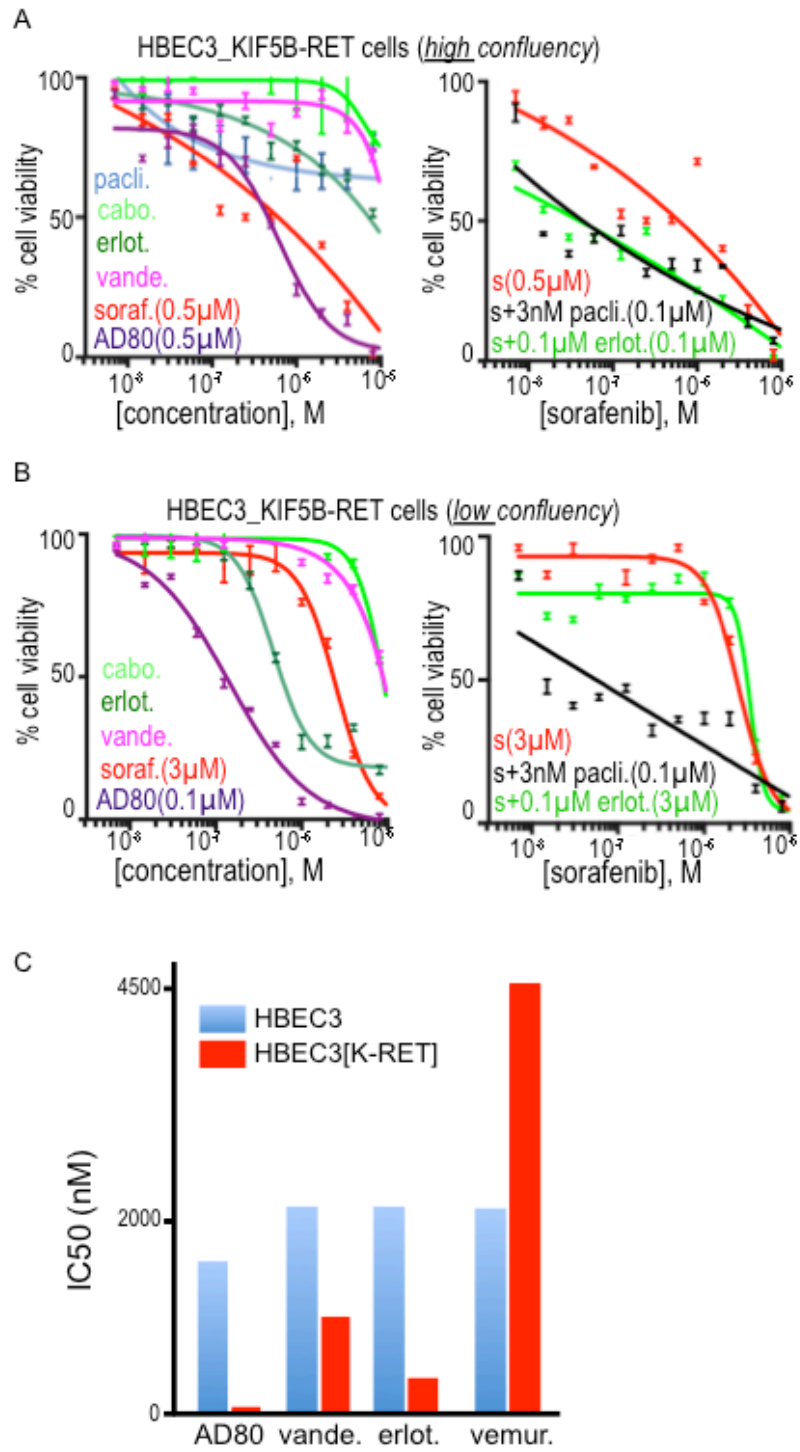
List of FDA-approved drugs used to screen KIF5B-RET flies

| Drug | Target | Marketed Name | Drug | Target | Marketed Name |
|---------------------------|----------------------------------|---------------|------------------------|----------------------------------|---------------|
| Abiraterone acetate(25µM) | Steroid CYP | Zytiga | Nelarabine(200µM) | Purine nucleoside antimetabolite | Arranon |
| Afatinib (50µM) | EGFR/HER2+kinases | GILOTTRIF | Nilotinib(25µM) | Abl+kinases | Tasigna |
| Anastrozole (100µM) | Aromatase | ARIMIDEX | Pamidronate(75µM) | Bone resorption | Aredia |
| Axitinib (37.5µM) | VEGF/PDGF/c-KIT | Inlyta | Pazopanib(50µM) | VEGF/PDGF/c-KIT | Votrient |
| Bendamustine HC(200µM) | DNA crosslinker | Treanda | Pemetrexed DiNA(1µM) | DNA synthesis | Alimta |
| Bortezomib(1µM) | Proteasome | Velcade | Pomalidomide(50µM) | Thalidomide analog | POMALYST |
| Bosutinib(200µM) | SRC/Abl+kinases | Bosulif | Ponatinib(50µM) | Bcr-Abl+kinases | Iclusig |
| Busulfan(200µM) | DNA crosslinker | Busulfex | Rapamycin(1µM) | mTOR+kinases | Rapamune |
| Cabazitaxel(20µM) | Microtubule | Jevtana | Regorafenib(50µM) | Ret+kinases | Stivarga |
| Cabozantinib(100µM) | Ret+kinases | CABOMETYX | Sorafenib(200µM) | Ret+kinases | Nexavar |
| Capecitabine(200µM) | DNA synthesis | Xeloda | Sunitinib Malate(50µM) | Ret+kinases | Sutent |
| Carfilzomib(50µM) | Proteasome | KYPROLIS | Tamoxifen(100µM) | Estrogen receptor | Nolvadex |
| Cinacalcet(100µM) | Calcimimetic | Sensipar | Temsirolimus(1µM) | mTOR+kinases | Torisel |
| Clofarabine(20µM) | Purine nucleoside antimetabolite | Clolar | Topotecan HCL(1µM) | Topoisomerase | Hycamtin |
| Crizotinib(50µM) | ALK/ROS+ kinases | Xalkori | Trametinib(1µM) | MEK+kinases | MEKINIST |
| Dabrafenib(100µM) | BRAF+kinases | Tafinlar | Vandetanib(25µM) | Ret+kinases | Caprelsa |
| Dasatinib(10µM) | SRC/Abl+kinases | Sprycel | Vemurafenib(50µM) | RAF+kinases | Zelboraf |
| Docetaxel(50µM) | Microtubule | Docetaxel | Vismodegib(1µM) | Smoothened Receptor | Erivedge |
| Doxorubicin(200µM) | DNA intercalator | Doxil | Vorinostat(10µM) | HDAC | Zolinsa |
| Epirubicin(200µM) | DNA intercalator | Ellence | Zoledronic Acid(7µM) | unknown | Zometa |
| Enzalutamide(100µM) | Androgen receptor | XTANDI | Ibrutinib(100µM) | BTK+kinases | IMBRUVICA |
| Erlotinib(25µM) | EGFR+kinases | Tarceva | Idelalisib(200µM) | p110d | ZYDELIG |
| Everolimus(1µM) | mTOR+kinases | Afinitor | Belinostat(200µM) | HDAC | Beleodaq |
| Exemestane(50µM) | Aromatase | Aromasin | Certinib(25µM) | ALK+kinases | ZYKADIA |
| Flutamide(100µM) | Androgen receptor | Eulexin | Nintendanib(10µM) | PDGFR/VEGFR/FGFR+kinases | Ofev |
| Fulvestrant(200µM) | Estrogen receptor | Faslodex | Olaparib(150µM) | PARP | LYNPARZA |
| Gefitinib(10µM) | EGFR+kinases | Iressa | Lenvatinib(50µM) | Ret+Kinases | LENVIMA |
| Gemcitabine(1µM) | Nucleoside analog | Gemzar | Panobinostat(200µM) | HDAC | Farydak |
| Imatinib(50µM) | Abl/PDGFR/c-KIT+kinases | Gleevec | Palbociclib(50µM) | CDK4,6 | Ibrance |
| Irinotecan(100µM) | Topoisomerase I | Camptosar | Ruxolitinib(200µM) | JAK+kinases | Jakafi |
| Lapatinib(100µM) | HER2/EGFR+kinases | Tykerb | Alectinib(0.05µM) | ALK+kinases | ALECNSA |
| Lenalidomide(200µM)) | Thalidomide analog | Revlimid | Vincristine(0.5µM) | microtubule | Marqibo |
| Letrozole(100µM) | Aromatase | Femara | Paclitaxel(0.5µM) | microtubule | Abraxane |
| | | | AD80(50µM) | Ret+Kinases | |

Suppl. Figure 6. Related to Figure 7.

Suppl. Figure 6. Related to Figure 7.

The panel of FDA approved drugs used to screen in *ptc>KIF5B-RET* flies. Also included: each drug's established primary in-vivo targets, and marketed brand name. Each drug was tested at a previously established *Drosophila* maximum tolerated dose (MTD). The doses are indicated and ranged, based on drug type, from 0.5 μ M to 400 μ M final concentration in fly food.



Suppl. Figure 7. Related to Figure 7.

Suppl. Figure 7. Related to Figure 7.

(A-C) Effect of drugs as single agents and as combinations on *HBEC3[KIF5B-RET]* cells. (A) Cells grown to *high* confluency. Dose response curve fitted to non-linear regression model using PRISM software; IC₅₀'s shown in brackets. Left Panel: confluent cells showed little sensitivity to clinically approved RET inhibitors vandetanib or cabozantinib (IC₅₀'s >10 μM), but cells showed sensitivity to both sorafenib and AD80 (IC₅₀s = ~0.5 μM). EGFR inhibitor erlotinib showed intermediate effect (IC₅₀ = ~10 μM). Right Panel: Combining sorafenib/erlotinib or sorafenib/paclitaxel potently inhibited (IC₅₀ = ~0.1 μM) growth of *HBEC3[KIF5B-RET]* cells. Paclitaxel (3 nM) or erlotinib (0.1 μM) alone—at doses used in combinations—had minimal detectable effect on growth of *HBEC3[KIF5B-RET]* cells (see Left Panel). (B) Cells grown to *low* confluency. Left Panel: low confluency cells showed little sensitivity to clinically approved RET inhibitors vandetanib, cabozantinib (IC₅₀s >10 μM). They showed moderate sensitivity to sorafenib (IC₅₀ = ~3 μM) and erlotinib (IC₅₀ = ~1 μM) and high sensitivity to AD80 (IC₅₀s = ~0.1 μM). Right Panel: Combining sorafenib/erlotinib did not show strong effect (IC₅₀ = ~3 μM) compared to sorafenib alone, but sorafenib/paclitaxel potently inhibited (IC₅₀ = ~0.1 μM) growth of *HBEC3[KIF5B-RET]* cells. (C) Column graph showing IC₅₀s of parental *HBEC3* and *HBEC3[KIF5B-RET]* cells. Dose response curves were performed as in panels A and B above and computed IC₅₀s were plotted as column graph. *HBEC3[KIF5B-RET]* cells showed increased sensitivity to AD80 and the EGFR inhibitor erlotinib compared to parental cells. Conversely *HBEC3[KIF5B-RET]* cells showed reduced sensitivity to the RAF inhibitor vemurafenib, indicating a switch away from dpERK signaling.